This is a preprint version of the paper published in

Journal of applied physics. The full-text final article may be downloaded from

J. Appl. Phys. 115, 243901 (2014) © 2014 AIP Publishing LLC

http://dx.doi.org/10.1063/1.4884610

Investigations of stacking fault density in perpendicular recording media

S.N. Piramanayagam, Binni Varghese, Yi Yang, Wee Kiat Lee and Hang Khume Tan

Data Storage Institute, A*STAR (Agency for Science, Technology and Research), 5, Engineering Drive 1, Singapore – 117608.

In magnetic recording media, the grains or clusters reverse their magnetization over a range of reversal field, resulting in a switching field distribution. In order to achieve high areal densities, it is desirable to understand and minimize such a distribution. Clusters of grains which contain a stacking fault have lower anisotropy, an order lower than those without stacking faults. It is believed that such low anisotropy regions reverse their magnetization at a much lower reversal field than the rest of the material with a larger anisotropy. Such clusters/grains cause recording performance deterioration such as adjacent track erasure and dc noise. Therefore, the observation of clusters that reverse at very low reversal fields

(nucleation sites) could give information on the noise and the adjacent track erasure. Potentially, the observed clusters could also provide information on the stacking faults (SF). In this paper, we study the reversal of nucleation sites in granular perpendicular media based on a magnetic force microscope (MFM) methodology and validate the observations with high resolution cross-section transmission electron microscopy (HRTEM) measurements. Samples, wherein a high anisotropy CoPt layer was introduced to control the nucleation sites (NS) or stacking faults (SF) in a systematic way, were evaluated by MFM, TEM and magnetometry. The magnetic properties indicated that the thickness of the CoPt layer results in an increase of nucleation sites. TEM measurements indicated a correlation between the thickness of CoPt layer and the stacking fault density. A clear correlation was also observed between the MFM results, TEM observations and the coercivity and nucleation field of the samples, validating the effectiveness of the proposed method in evaluating the nucleation sites which potentially arise from stacking faults.

Corresponding author: prem_SN@dsi.a-star.edu.sg

1. Introduction

Granular perpendicular recording media based on stacked layers of CoCrPt:Oxide are currently used in hard disk drives.[1,2] The layers are designed in such a way that the bottom most layer has the highest anisotropy constant, which helps to achieve the desired thermal stability for the whole stack of recording layer grains.[3,4] The layers on top have gradually reduced values of anisotropy constant. The magnetic layers with different anisotropy are separated by some non-magnetic layers to fine tune the exchange coupling between them. [5] Such a design helps in switching of the whole stack through an incoherent reversal process, which enables a writing process at a lower field than that is required in the case of coherent reversal mechanism.[6,7] The bottom layer with the highest anisotropy constant has a large amount of Pt and plays a key role in the thermal stability.[8] Although thermal stability can be increased by increasing the Pt concentration to certain extent, it is commonly known that the addition of Pt in excess of 20 at% causes stacking faults.[9,10] Since the variation in Pt concentration from grain to grain in the deposited film cannot be controlled precisely, the stacking fault density will increase if Pt concentration is increased beyond 20 at%. As the grains with the stacking faults have a much lower anisotropy, they widen the switching field distribution and cause dc erase noise and adjacent track erasure issues.[11] Therefore, the Pt concentration in recording media is typically kept at a value less than 20 at% (besides cost consideration).[12] In order to achieve higher anisotropy in CoPt systems with Pt concentrations higher than 20 at%, it is essential to establish methods which can give an estimation of stacking fault density in a straightforward manner.

In longitudinal recording media, the stacking faults lie perpendicular to the disk surface and hence a plane view transmission electron microscopy (TEM) could provide visual information of the density of stacking faults in a given area.[13] However, in perpendicular recording media, the stacking faults lie along the film-plane and hence cross-section TEM

provides information about stacking faults.[14,15] However, the information from cross-section TEM are statistically insufficient. Therefore, it is essential to identify suitable methods which can provide an estimation of stacking fault densities as was possible during the era of longitudinal recording media. In this study, we have made a special set of samples with various amount of stacking faults and have characterized them using a new magnetic force microscope (MFM) methodology.

2. Experimental Details

The samples for this study were prepared on glass disk substrates by dc magnetron sputtering using Intevac Lean 200 production type sputtering machine. Typical seedlayers, which are used for achieving hcp(00.2) texture in Co-alloy layer, were deposited prior to the deposition of the CoCrPt:oxide recording layer.[16] The recording layer was covered with a capping layer and a carbon overcoat.[17] The thickness of the granular CoCrPt:oxide layer was kept at 10 nm, slightly thinner than the typical total thickness of recording media. The samples were characterized using polar Kerr magnetometry (MOKE), transmission electron microscopy (TEM), X-ray diffraction (XRD) and MFM. A CoPt layer with a near-equiatomic Pt concentration (called stacking fault inducing layer, SFI) which increases the stacking faults with an increase of thickness due to the high Pt concentration, was introduced below the CoCrPt:Oxide recording layer. Figure 1 shows a schematic of the recording media layer structure. Figure 1(b) shows the XRD patterns of samples with different SFI layer thicknesses. It can be noticed from figure that the samples show peaks corresponding to the Ru seedlayer and the Co alloy layer at around 42.4 and 43.2 degrees, respectively. An fcc(111) peak induced by the SFI layer, corresponding to the stacking faults, emerges at around 41.4 degrees in samples with thicker SFI layer, indicating that the SFI layer carries out its proposed function of producing grains/clusters with lower anisotropy, probably through the formation of stacking faults.

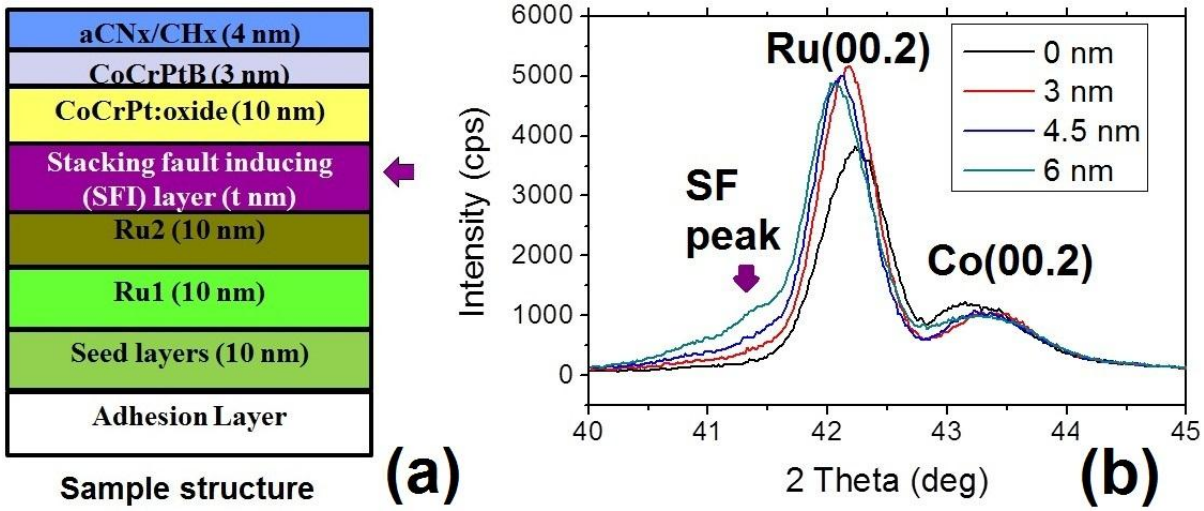

Figure1: (a) A sketch of the media layer structure with approximate thicknesses. (b) XRD patterns of samples with different SFI layer thicknesses.

3. Methodology

In granular perpendicular recording media, the stacking faults have been characterized using synchrotron XRD techniques or cross-section TEM methods.[18] In cross-section TEM, the number of grains that can be seen in order to spot the stacking faults is very few. Therefore, cross-section TEM technique is not statistically sufficient. Synchrotron XRD has been used to measure the stacking faults.[19] Quite recently, laboratory based XRD also has been used to measure the stacking fault density.[20] Although XRD method is suitable for CoPt alloys with Pt concentration less than 30 at%, a specific problem to XRD arises for near-equiatomic CoPt, particularly when the peaks of CoPt and Ru overlap with each other. Even though the "c" lattice parameter of Co is lower than that of Ru, addition of Pt leads to an increase in the lattice parameter, resulting in an overlap of hcp(00.2) peaks. Considering the drawbacks of these existing techniques, we have attempted investigating if stacking faults could be visualized using a simple but effective technique based on MFM. As MFM scan does not involve any special sample preparation and does not take more than an hour, this method has

potential advantages when many samples need to be investigated. In this study, we have hypothesized that the grains or clusters with stacking faults will reverse at much lower reversal fields due to their lower anisotropy than those without stacking faults. Such a reversal could happen even at remanence, in samples with a higher saturation magnetization than that of our samples due to higher magnetostatic fields. Therefore, observation of clusters that reverse at lower fields or even at remanence (nucleation sites) could potentially give information on the stacking faults, although care needs to be taken in interpreting this information. Therefore, we have also carried out cross-section TEM to validate the observations.

MFM has been traditionally used to measure recorded bit-patterns of a recording medium.[21] It has also been used to measure the cluster sizes in an AC demagnetized (ACD) state.[22] ACD has also been used to measure the magnetic roughness.[23] Useful correlation has been identified between the noise of the recording media and cluster sizes or magnetic roughness. However, MFM has not been used much to image nucleation sites arising from stacking faults or other sources. In our MFM methodology, we saturated the samples first and then applied a small reversal field (typically less than the nucleation field of the sample ~ about 1000 Oe in the case of CoCrPt-based perpendicular media). Subsequently, the field was reduced to zero and samples were moved to the MFM stage and MFM was carried out at remanence. Figure 2 is an illustration of the methodology, which also shows an example of MFM image of a sample in this study with reversed nucleation sites (which are potentially due to stacking faults) as highlighted by dark circle.

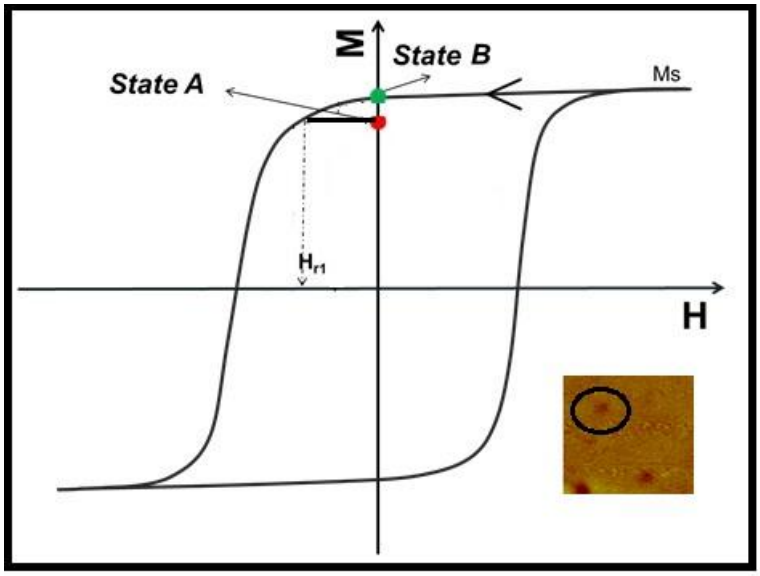

Figure 2: (a) Schematic illustration of the magnetic states at which MFM measurements were carried out. State A represents measurement at remanence after the application of a reversal field H_{r1}, which is a fraction of H_n. State B represents measurement at remanence after saturation (Inset) Typical MFM image of a media sample with reversed captured at the State A. The circled regions and similar (uncircled) dots are the reversed regions most probably due to stacking faults.

4. Results and Discussion

Figure 3 shows the hysteresis loops and other magnetic properties as obtained from MOKE magnetometry. It can be noticed from figure 3(a) that the reference sample has an H_c and H_n of about 4500 and 1500 Oe respectively. When the SFI layer with a thickness of 3 nm was introduced, the H_n and H_c improved considerably to 4900 and 2300 Oe respectively. From our previous studies on CoPt layer material using TEM and magnetic characterization techniques, it is known that the CoPt layer does not cause significant stacking faults at this thickness.[24] Moreover, it also does not cause any increase of exchange coupling between the grains. As a result, the increase in anisotropy energy (K_uV) leads to an increase of H_c and H_n induced by the SFI layer at this thickness. It must be mentioned that the increase in anisotropy might come from increased K_u of the SFI layer, increase in V of the grain due to

the increased thickness or both. However, the sample with a 6 nm SFI layer shows a lower H_c (4000 Oe) and H_n (1700 Oe), despite the increased volume. Although the low H_n observed in this sample (as compared to the sample with 3 nm SFI layer) is believed to be due to the reduction in K_u arising from stacking faults, the increase in exchange coupling between the grains of SFI layer is probably another source of reduction in H_n and H_c. Even though the SFI layer was sputtered at high pressures, it did not have segregants and hence it is expected to increase exchange coupling in thicker layers. It should, however, be noted that any minor increase in exchange coupling (as by a cap layer in perpendicular media) would only increase the nucleation field. Therefore, the decrease of H_n in sample with 6 nm SFI layer is most likely due to the increased number of stacking faults at this thickness.

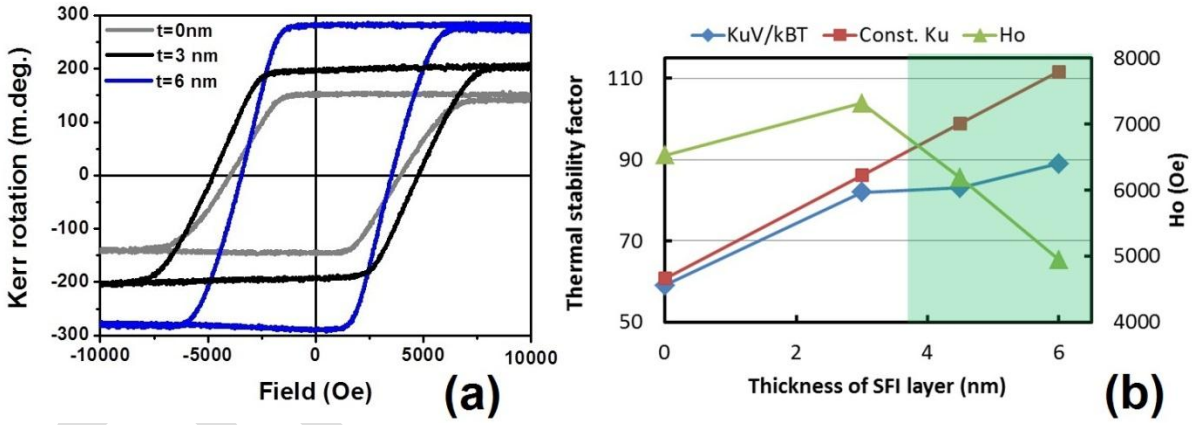

Figure 3: (a) MOKE hysteresis loop of the samples with different SFI layer thickness. (b) Estimated values of anisotropy field (H_o) and the thermal stability factor (K_uV/k_BT) (from dynamic coercivity), as a function of SFI layer thickness. Variation of thermal stability with SFI layer thickness for a constant K_u value of $7x10^6$ erg/cc is also shown.

Time-dependent MOKE measurements (dynamic remanent coercivity) were carried out in order to gain further understanding on the magnetic properties of these samples. The scanning time was varied from 10s to 100s in 5 steps. The data were fitted to Sharrock's equation and the R^2 of the fitting was about 0.99. R^2 close to 1 indicates that the data from MOKE were good enough to obtain information on the anisotropy field (H_o) and the thermal stability

factor (K_uV/k_BT) (shown in Figure 3(b)).[25] The ideal K_uV/k_BT, (assuming a constant K_u of $7x10^6$ erg/cc for the scenario that the SFI layer did not have any stacking faults), is also plotted together. It can be noticed that the K_uV/k_BT increases with the introduction of SFI layer. However, the increase is not seen to be along the expected lines, except for sample with 3 nm thick SFI layer. For samples with thicker SFI layer, the increase of K_uV/k_BT happens at a much slower rate than the ideal value. In unison, H_o shows the highest value for SFI layer thickness of 3 nm. For further increase of SFI layer, H_o decreases. These results indicate that the introduction of SFI layer beyond 3 nm causes stacking faults, which leads to a reduction in the anisotropy constant of those grains with stacking faults. Since H_o and K_uV/k_BT are measured from the time-dependent coercivity (from the magnetization reversal of about 50% grains), they do not provide an accurate picture of the stacking faults. However, as the number of the grains with stacking faults is expected to be only a small fraction of the whole material, they do provide a signature effect of grains with stacking faults. The results from figure 3 are an indication that the stacking faults, although occur at 3 nm thickness, increase significantly with SFI thickness beyond 3 nm.

Figure 4(a) shows the MFM images and the number of clusters measured as a function of SFI layer thickness. The reversed clusters, in dark brown color, can be seen from figure 4(a). The diameter of the clusters measured from the MFM images in samples with thinner SFI is about 50 nm. It must be mentioned that the size of reversed clusters in MFM images is typically larger than the actual magnetic dots (or clusters). In patterned media with 30 nm dot sizes, the reversed dots in MFM were observed to have a size of about 70 nm.[26] Therefore, these clusters may have an actual size of 20-30 nm. These results confirm our hypothesis for this work that, under the application of a small reversal field, the clusters with a low thermal stability (due to stacking faults or for compositions that result in a very low anisotropy)

reverse their magnetization and appear in MFM and that the reversal at a small reversal field (around 1000 Oe) is not due to the small grains.

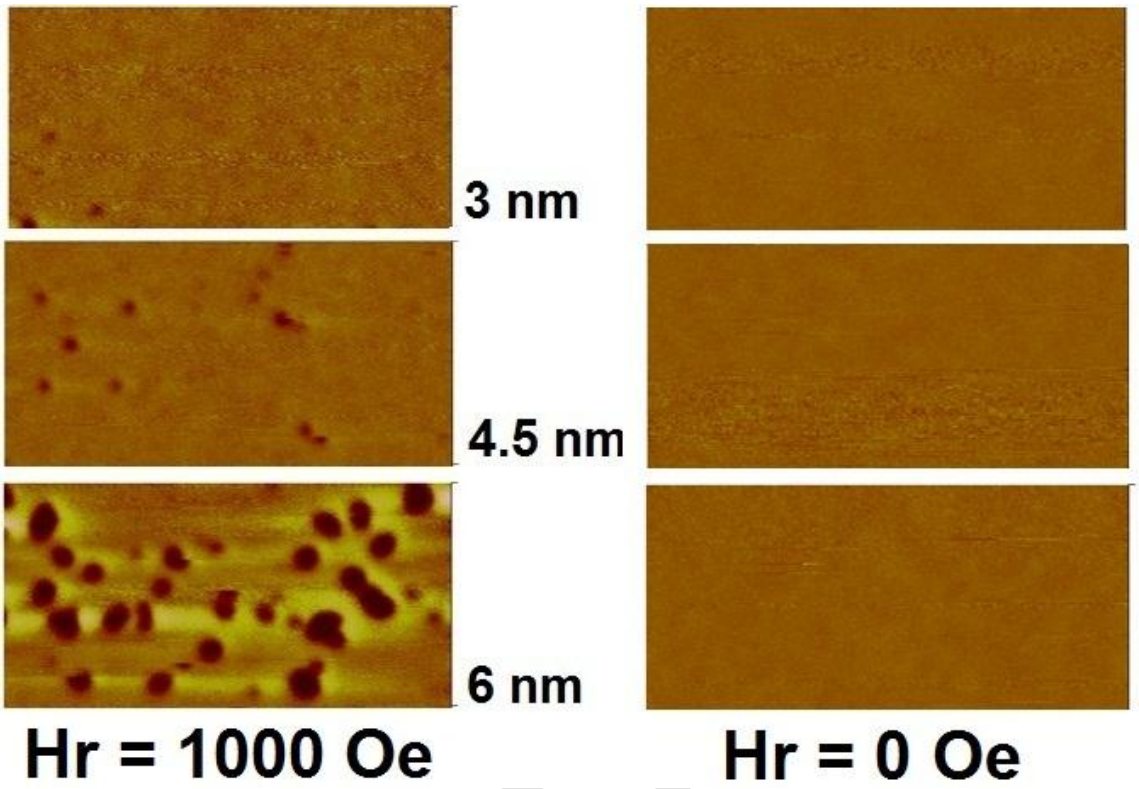

Figure 4: MFM images of the samples with different SFI layer thicknesses, measured at a reverse field (Hr) of 1000 Oe and 0 Oe.

To illustrate this point further, we provide a simple calculation based on an isolated CoPt cluster with a diameter of 20 nm and a thickness of 10 nm. If all the grains in this cluster of CoPt are in hcp phase, the cluster would have a thermal stability factor of about 380 and it could not be reversed by a small reversal field (Since H_k of such a cluster is more than 10 kOe). On the other hand, if this cluster has a stacking fault, its anisotropy would be reduced by a factor, resulting in a thermal stability factor of only about 38 (Clusters with diameters in the range of 20-25 nm, would have a thermal stability factor between 40 and 60). Such clusters would flip their magnetization at a small reversal field due to the thermal effects. An hcp grain of 6 nm diameter will also have similar thermal stability factor value, but such a

grain may not be observable within the resolution limit of MFM (about 20 nm) when its magnetization is flipped. In essence, the clusters that show up in MFM for small reversal fields are more likely arising from grains with a lower anisotropy constant (due to stacking faults, for example) than entirely due to changes in volume of grains. Figure 4(b) shows the same set of samples, which were measured at state B, which is at remanence after a saturating field was applied and removed. They do not show any reversed clusters, indicating that the nucleation sites due to SF or low anisotropy grains must be measured at a suitable reversal field, depending on the nature of the sample. It can also be noticed from figure 4(a) that the number of clusters increases as a function of SFI thickness.

Figure 5 shows the number of reversed clusters for different samples, plotted as a function of SFI thickness. The H_c and H_n values of the samples are also shown in figure 5, which show an opposite trend, as compared to the number of reversed clusters. In conjunction with the magnetometry results, such as K_uV/k_BT, H_o, H_c and H_n, the MFM results indicate that the nucleation sites due to stacking faults increase as the SFI layer thickness increases from 3 to 6 nm. From figure 4, it was noticed that the size and contrast of the clusters also increase as a function of thickness. This is due to the increase in exchange coupling, as the thickness of SFI layer was increased. Although the SFI layer was sputtered at higher pressures to achieve a segregated structure, this layer did not have the usual oxide segregants. As a result, the decoupling between the grains deteriorated as thickness increased. This is further confirmed by the increase of dM/dH with thickness of SFI layer in figure 5 (as measured from the slope near coercivity of MOKE hysteresis loops).

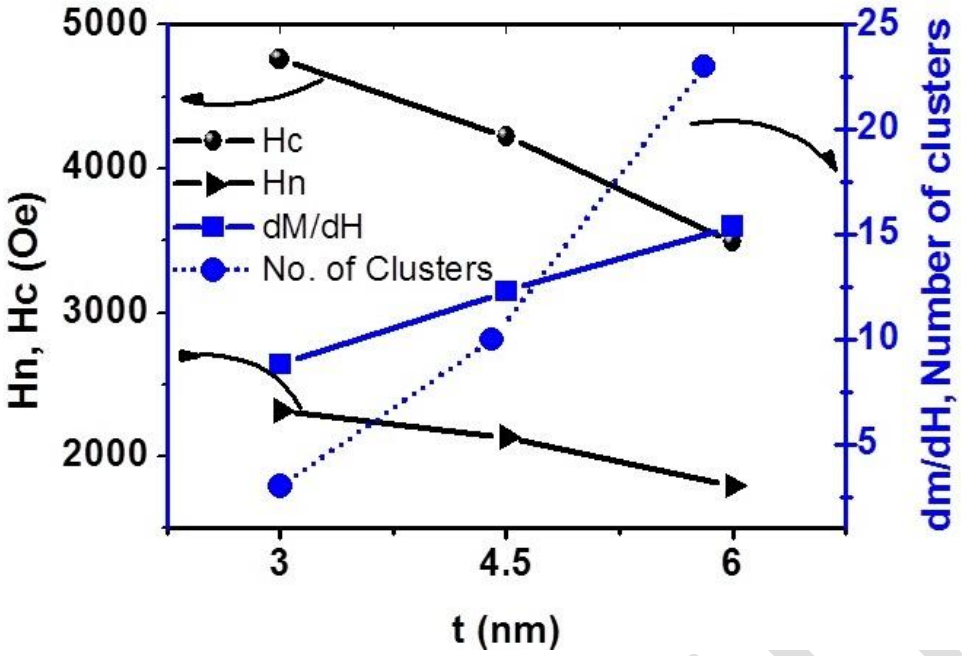

Figure 5: Effect of SFI layer thickness on the coercivity, nucleation field, dM/dH and number of clusters observed in MFM.

Although the trends discussed in figure 5 more or less establish the fact that the stacking faults could be estimated from MFM, it is useful to validate this observation further by carrying out additional measurements. Although TEM measurement is not as fast as the MFM measurement, it provides clearer evidence of the stacking faults. Detailed HRTEM measurements were carried out to find out the microstructure properties of CoCrPt and CoPt. Figure 6 (a) and (b) show the TEM images of samples with 3 and 6 nm of SFI layer thickness, respectively, focussed at SFI and CoCrPt layers. In the case of sample with 3 nm SFI layer, no significant stacking fault could be found in the SFI layer, and the CoCrPt layer growing on top of it shows stacking faults (indicated by blue arrows). On the other hand, in the case of sample with 6 nm SFI layer, much more significant number of stacking faults can be observed in CoPrPt layer as indicated by blue arrows. In both samples, a region of fcc phase can be found at the CoCrPt/CoPt interface, and phase transformation from hcp to fcc and vice versa happens. The fcc phase has an order lower anisotropy in comparison to that in

hcp phase. The thickness of this fcc phase increases with the increase of CoPt layer thickness, which is in consistence with increased number of clusters observed in MFM analysis. the top portion of the layer exhibits a phase transformation from hcp to fcc structure. The CoCrPt layer that grows on top of such a grain exhibits stacking faults.

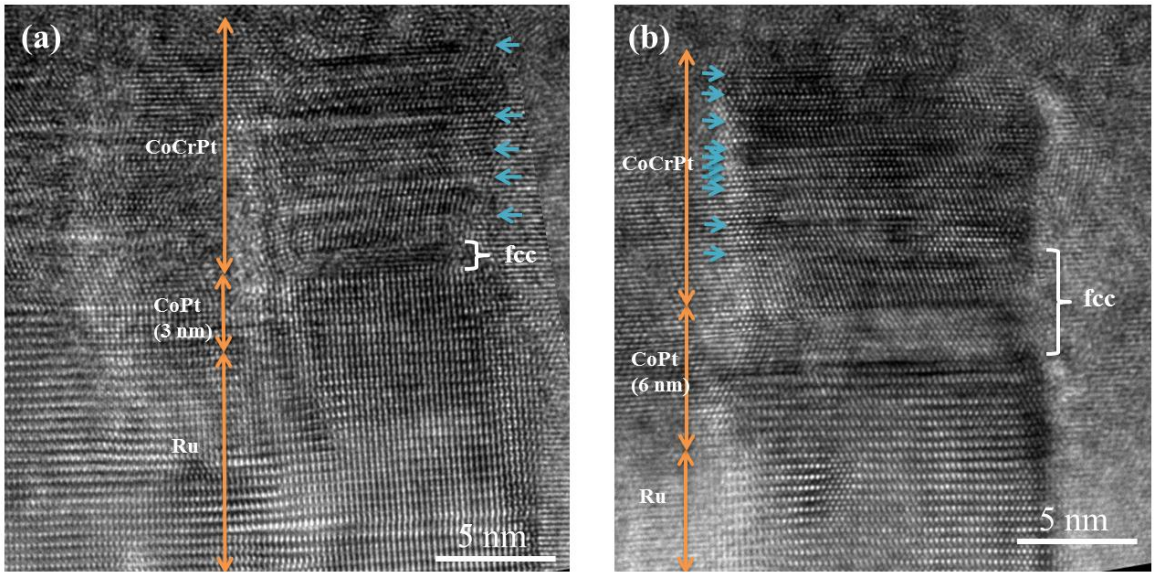

Figure 6. Typical cross-section TEM images of SFI-CoPt(t nm)/CoCrPt:Oxide (10 nm) samples with (a) 3 nm SFI layer and (b) 6 nm SFI layer.

Figure 7 shows a plot of the number of MFM clusters in the samples as a function of the stacking faults observed in the same set of samples. Although there is a correlation between the two, the trend is not linear. This can be understood from the fact that the MFM measures the number of clusters in a given area (L^2) and the cross-section TEM measures the number of clusters in a scale of length (L). In addition, it was reported that the Ku for pure Co film can be reduced by more than a factor of 2 due to increase of 10% of the hcc phase,[27] which indicates the fcc phase or the stacking fault can largely alter the K_u value. Therefore, the quadratic increase of MFM clusters (as compared to the TEM cross-section clusters) is expected. It must also be mentioned that in order to make our observation representative, the

several MFM and TEM measurements were carried out and the average number of clusters (or stacking faults) was considered in both cases. These results indicate the correlation between the MFM clusters and the stacking faults, as observed by cross-section TEM.

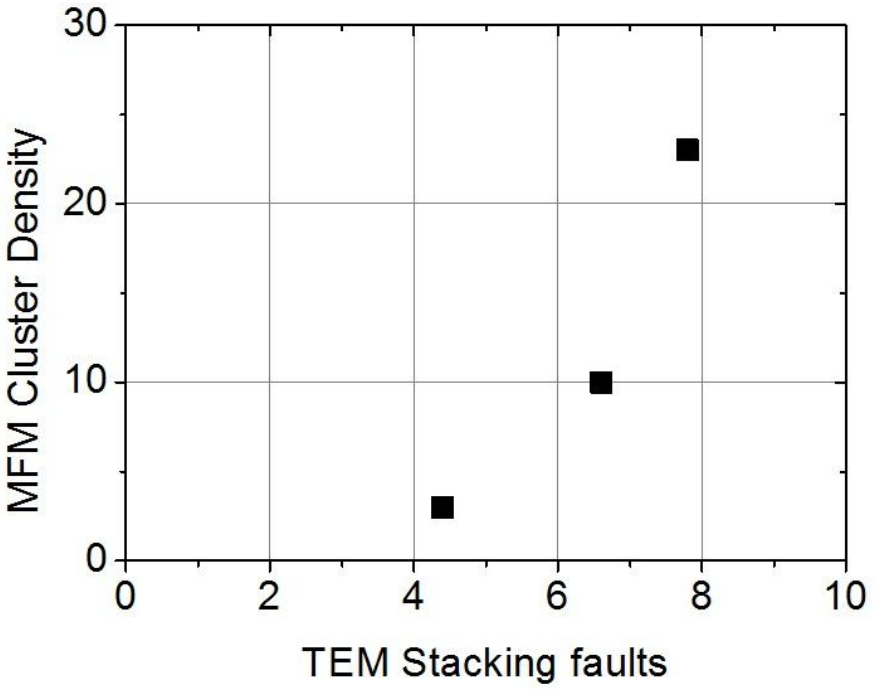

Figure 7. Correlation between the MFM cluster density and the number of stacking faults measured using cross-section TEM

5. Conclusions

As a conclusion, we have proposed the use of measuring clusters that reversed their magnetization at small reversal fields as a method to study stacking faults. Our studies on samples with stacking faults indicates a clear correlation between the number of reversed clusters in MFM and the coercivity and nucleation field of the samples indicating the effectiveness of the method. Validation of the MFM results was achieved using TEM observation of stacking faults. Although MFM is not a direct method for visualizing stacking

faults, the proposed method is useful for the recording media applications in estimating the density of grains with stacking faults.

References

[1] S. N. Piramanayagam, J. Appl. Phys., **102,** 011301 (2007).

[2] H. J. Richter, J. Magn. Magn. Mater., **321** 467 (2009).

[3] D. Suess, Appl. Phys. Lett., **89**, 113105 (2006).

[4] S.N. Piramanayagam, J.Z. Shi, H.B. Zhao, C.S. Mah and J. Zhang, IEEE Trans. Magn., **41(10)** 3190 (2005).

[5] J.G. Zhu and Y.M. Wang, IEEE Trans. Magn., **47(10)** 4066 (2011).

[6] J. -P. Wang, W. K. Shen, J. M. Bai, R. H. Victora, J. H. Judy, and W. L. Song, Appl. Phys. Lett., **86,** 142504 (2005).

[7] N. Gaur, K. K. M. Pandey, S. L. Maurer, S. N. Piramanayagam, R. W. Nunes, H. Yang, and C. S. Bhatia, J. Appl. Phys., **110,** 083917 (2011).

[8] H. Yuan and D. E. Laughlin, J. Appl. Phys., **105,** 07A712 (2009).

[9] T. Kubo, Y. Kuboki, M. Ohsawa, R. Tanuma, A. Saito, T. Oikawa, H. Uwazumi, and T. Shimatsu, J. Appl. Phys., **97,** 10R510 (2005).

[10] T. Shimatsu, H. Sato, T. Oikawa, Y. Inaba, O. Kitakami, S. Okamoto, H. Aoi, H. Muraoka, and Y. Nakamura, IEEE Trans. Magn., **41,** 566 (2005).

[11] J. –G. Zhu, X. Zhu, Y. Tang, IEEE Trans. Magn., **44,** 125 (2008).

[12] N. Nozawa, S. Saito, S. Hinata, M. Takahashi, J. Phys. D: Appl. Phys., **46** 172001 (2013)

[13] D.E. Laughlin, B. Lu, Y-N. Hsu, J. Zou, and D.N. Lambeth, IEEE Trans. Magn., **36(1)** 48 (2000).

[14] M. Zheng, G. Choe, A. Chekanov, B. G. Demczyk, B. R. Acharya, and K. E. Johnson, IEEE Trans. Magn., **39(4)** 1919 (2003)

[15] B. Lu, T. Klemmer, K. Wierman, G. P. Ju, D. Weller, A. G. Roy, D.E. Laughlin, C. H. Chang, and R. Ranjan, J. Appl. Phys., **91,** 8025 (2002).

[16] S. N. Piramanayagam, K. Srinivasan, J. Mag. Mag. Mater., **321,** 485 (2009).

[17] G. Choe, M. Zheng, B.R. Acharya, E.N. Abarra, J.N. Zhou, IEEE Trans. Magn., **41(10)** 3172 (2005).

[18] Y. Takahashi, K. Tanahashi, and Y. Hosoe, J. Appl. Phys., 91, 8022 (2002).

[19] H.S. Jung et al., IEEE Trans. Magn., **43(2),** 615 (2007).

[20] S. Saito, A. Hashimoto, D. Hasegawa, and M. Takahashi, J. Phys. D: Appl. Phys., **42,** 145007, (2009).

[21] M. Futamoto et al., IEEE Trans. Magn., **49(6),** 2748, (2013)

[22] Murayama A., Hyomi K., Ohshima K., Miyamura M., Maekawa M., Kondoh S., J. Appl. Phys., **81 (8),** 3925 (1997).

[23] Glijer P., Sivertsen J. M., Judy J. H., IEEE Trans. Magnetics, **31**, 2842 (1995).

24 B. Varghese, S.N. Piramanayagam, Y. Yang, S.K. Wong, H.K. Tan, W.K. Lee and I. Okamoto, J. Appl. Phys., **115**, 17B707 (2014)

25 M. P. Sharrock, J. Appl. Phys., **76**, 6413 (1994).

[26] M. Ranjbar, A. Tavakkoli, S.N. Piramanayagam, K.P. Tan, R. Sbiaa, S.K. Wong and T.C. Chong, J. Phys. D: Appl. Phys., **44** 265005 (2011)

[27] S. Hinata, R. Yanagisawa, S. Saito and M. Takahashi, J. Appl. Phys., **105**, 07B718 (2009)